

A Statistical Model for the Excitation of Cavities Through Apertures

Gabriele Gradoni, *Member, IEEE*, Thomas M. Antonsen, *Fellow, IEEE*, Steven M. Anlage, *Member, IEEE*, and Edward Ott, *Life Fellow, IEEE*

Abstract—In this paper, a statistical model for the coupling of electromagnetic radiation into enclosures through apertures is presented. The model gives a unified picture bridging deterministic theories of aperture radiation, and statistical models necessary for capturing the properties of irregular shaped enclosures. A Monte Carlo technique based on random matrix theory is used to predict and study the power transmitted through the aperture into the enclosure. Universal behavior of the net power entering the aperture is found. Results are of interest for predicting the coupling of external radiation through openings in irregular enclosures and reverberation chambers.

Index Terms—Admittance matrix, aperture coupling, cavities, chaos, reverberation chamber (RC), statistical electromagnetics.

I. INTRODUCTION

THE coupling of electromagnetic (EM) radiation into enclosures or cavities through apertures both electrically small [1] and large [2] has attracted the interest of the EM community for many years [3], [4]. Full solutions of this problem are particularly complicated because of the mathematical complexity in the solution of the boundary-value problem and because of the sensitivity of the solution to the detail of the enclosure's dimensions, content, and the frequency spectrum of the excitation. These difficulties have motivated the formulation of a statistical description, known as the random coupling model (RCM) [5]–[7], of the excitation of cavities. The model predicts the properties of the linear relation between voltages and currents at ports in the cavity, when the ports are treated as electrically small antennas.

In this paper, we formulate and investigate the RCM as it applies to cases in which the ports are apertures in cavity walls. The aperture is assumed to be illuminated on one side by a plane EM wave. We then distinguish between the radiation problem, where the aperture radiates into free space, and the cavity problem, where the aperture radiates into a closed EM environment. The solution of the problem in the cavity case is then given in

Manuscript received February 28, 2014; revised October 14, 2014; accepted November 14, 2014. Date of publication July 23, 2015; date of current version October 12, 2015. This work was supported by the Air Force Office of Scientific Research FA95501010106 and the Office of Naval Research N00014130474.

G. Gradoni, T. M. Antonsen, and E. Ott are with the Institute for Research in Electronics and Applied Physics, University of Maryland, College Park, MD 20742 USA (e-mail: ggradoni@umd.edu; antonsen@umd.edu; edott@umd.edu).

S. M. Anlage is with the Center for Nanophysics and Advanced Materials, University of Maryland, College Park, MD 20742 USA (e-mail: anlage@umd.edu).

Color versions of one or more of the figures in this paper are available online at <http://ieeexplore.ieee.org>.

Digital Object Identifier 10.1109/TEMC.2015.2421346

terms of the free-space solution and a fluctuation matrix based on random matrix theory (RMT). Thus, there is a clear separation between the system specific aspects of the aperture, in terms of the radiation admittance, and the cavity in terms of the fluctuation matrix.

We illustrate our method by focusing on the problem of an electrically narrow aperture, for which the radiation admittance can be easily calculated numerically. We then generalize our result to the interesting case, where a resonant mode of the aperture is excited. In this case, the statistical properties of the aperture-cavity system can be given in a general universal form.

Our results build on previous work on apertures. In particular, rectangular apertures have a very long research tradition in EM theory [3], and continue to be a topic of interest [8]. The first self-consistent treatments have been carried out by Bethe [1], Bouwkamp [9], and, later, by Schwinger in aperture scattering [10], and Roberts [11]. Subsequent work on apertures is due to Ishimaru [12], Cockrell [13], Harrington [2], [3], [14], [15], and Ramat-Sahmii [4], [16], among other investigators.

Our results are of interest for the physical characterization of the radiation coupled into complex cavities such as reverberation chambers (RC)—which is known to be an extremely complicated problem even challenging classical electromagnetic compatibility (EMC) techniques [17]–[19]—for understanding interference in metallic enclosures, as well as for modeling and predicting radiated emissions in complicated environments.

This paper is organized as follows. In Section II, we introduce the general model for the cavity-backed aperture, and we describe the way the RCM models the cavity. In Section III, we apply the formulation of Section II to large aspect ratio, rectangular apertures; evaluating the elements of the admittance matrix and computing the power entering a cavity with a rectangular aperture. In this section, we also develop a simple formula for the power entering a low-loss cavity with isolated resonances. Section IV describes an extension of the model that accounts for the coupling of power through an aperture, into a cavity, and to an antenna in the cavity. Simple formulas for the high-loss case, low-loss, isolated resonance are developed.

II. RANDOM COUPLING MODEL FOR APERTURES

The random coupling model was originally formulated to model the impedance matrix of quasi-2D cavities with single [5], and multiple [6] point-like ports [7]. In this section, we develop the model for three-dimensional (3-D) *irregular* enclosures excited through apertures [20]. As depicted in Fig. 1, we consider a cavity with a planar aperture in its wall through which our complex EM system is accessed from the outside.

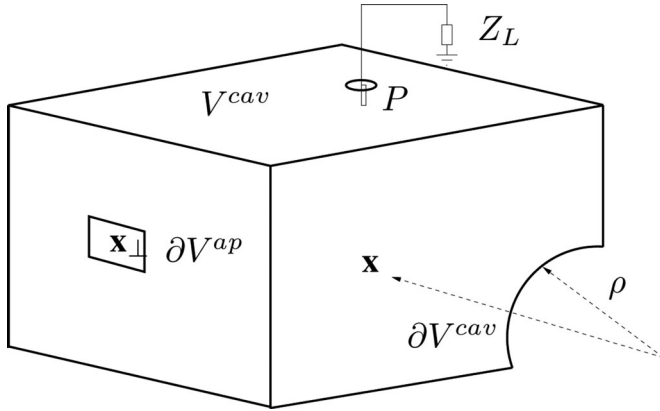


Fig. 1. Geometry of a complex 3-D cavity with volume V^{cav} , boundary ∂V^{cav} , exhibiting wave-chaotic ray trajectories in the semiclassical limit: energy enters the cavity through an electrically large aperture ∂V^{ap} . Also shown is a point-like port to be considered in Section IV.

The size and shape of the aperture are important in our model; their specification constitutes “system specific” information that is needed to implement the model. The cavity that we consider in our studies is an electrically large enclosure with an irregular geometry. The irregularity is assumed to be such that ray trajectories within the cavity are chaotic throughout [21]. Generally speaking, typical cavities have this feature; particularly, those with curved walls and/or with contents that scatter radiation in multiple directions. The consequences of assuming trajectories are chaotic is that the spectra of modes of the cavity have universal statistical properties that are modeled by RMT [22]. Experiments have been carried out to test the predictions of RCM for quasi-two-dimensional (2-D) complex enclosures coupled through electrically small (point-like) ports [23]–[25]. Experiments have also been carried out in 3-D enclosures, and with electrically large ports [26], [27].

When apertures are considered, the port approximation invoked in the original derivation of the RCM is no longer valid, hence we need to consider the field distribution on the aperture surface. We consider a planar aperture, i.e., one that is not subject to boundary curvature. This is consistent with real-world situations such as 3-D RCs [28], where the aperture is generally in a planar boundary. We henceforth assume that $\epsilon = \epsilon_0, \mu = \mu_0$ in all nonconducting regions of space.

We first treat the aperture as if it existed in a metal plate separating two infinite half-spaces. We refer to this as the “free-space” situation or “radiation” case. Suppose the port is treated as an aperture in a planar conductor whose surface normal \hat{n} is parallel to the z -axis. The components of the fields transverse to z in the aperture can be expressed as a superposition of modes (an example is the set of modes of a waveguide with the same cross-sectional shape as the aperture)

$$\mathbf{E}_t = \sum_s V_s \mathbf{e}_s(\mathbf{x}_\perp) \quad (1)$$

and

$$\mathbf{H}_t = \sum_s I_s \hat{n} \times \mathbf{e}_s(\mathbf{x}_\perp) \quad (2)$$

where \mathbf{e}_s is the basis mode, (having only transverse fields) normalized such that $\int d^2 \mathbf{x}_\perp |\mathbf{e}_s|^2 = N_s$ and \hat{n} is the normal, which we take to be in the z -direction. In the radiation case, we solve Maxwell’s equations in the half-space $z > 0$ subject to the boundary conditions that $\mathbf{E}_t = 0$ on the conducting plane except at the aperture, where it is given by (1). We do this by removing the conducting plane, adding a magnetic surface current density $2\delta(z) \hat{n} \times \mathbf{E}_t$ to Faraday’s law, and solving Maxwell’s equations in the whole space $-\infty < z < \infty$ in the Fourier domain. For this problem, the transverse components of the electric field are odd functions of z with a jump equal to twice (1) at the location of the aperture; thus satisfying the boundary condition for the half-space problem. We then evaluate the transverse components of the magnetic field on the plane $z = 0$, and project them on to the basis $\hat{n} \times \mathbf{e}_s(\mathbf{x}_\perp)$ at the aperture to find the magnetic field amplitudes I_s in (2). The result is a matrix relation between the magnetic field amplitudes and the electric field amplitudes in the aperture

$$I_s = \sum_{s'} Y_{ss'}^{\text{rad}}(k_0) V_{s'} \quad (3)$$

where $k_0 = \omega/c$, ω is the frequency of excitation and we have adopted the phasor convention $\exp(-i\omega t)$. Here, the radiation admittance matrix $Y_{ss'}^{\text{rad}}$ is determined from the Fourier transform solution for the fields, and is given in terms of a 3-D integral over wave numbers

$$Y_{ss'}^{\text{rad}}(k_0) = \sqrt{\frac{\mu}{\epsilon}} \int \frac{d^3 k}{(2\pi)^3} \frac{2ik_0}{k_0^2 - k^2} \tilde{\mathbf{e}}_s^* \cdot \Delta_{=Y^{\text{rad}}} \cdot \tilde{\mathbf{e}}_{s'} \quad (4)$$

where the dyadic tensor

$$\Delta_{=Y^{\text{rad}}} = \frac{\mathbf{k}_\perp \mathbf{k}_\perp}{k_\perp^2} + \left(\frac{k^2 - k_\perp^2}{k^2} + \frac{(k_0^2 - k^2) k_\perp^2}{k^2 k_0^2} \right) \frac{(\mathbf{k} \times \hat{n})(\mathbf{k} \times \hat{n})}{k_\perp^2} \quad (5)$$

is responsible for coupling two arbitrary modes of the aperture, and

$$\tilde{\mathbf{e}}_s = \int_{\text{aperture}} d^2 \mathbf{x}_\perp \exp(-i\mathbf{k}_\perp \cdot \mathbf{x}_\perp) \mathbf{e}_s \quad (6)$$

is the Fourier transform of the aperture mode. The elements of the radiation admittance are complex quantities. The residue at the pole $k = k_0$ in (4) gives the radiation conductance

$$G_{ss'}^{\text{rad}}(k_0) = \sqrt{\frac{\epsilon}{\mu}} \int \frac{k_0^2 d\Omega_k}{8\pi^2} \tilde{\mathbf{e}}_s^* \cdot \Delta_{=G^{\text{rad}}} \cdot \tilde{\mathbf{e}}_{s'} \quad (7)$$

where Ω_k is the 2-D solid angle of the wave vector \mathbf{k} to be integrated over 4π , and where there appears a modified dyadic tensor

$$\Delta_{=G^{\text{rad}}} = [(\mathbf{k}_\perp \mathbf{k}_\perp) / k_\perp^2] + [(\mathbf{k} \times \hat{n})(\mathbf{k} \times \hat{n}) / k_\perp^2] \quad (8)$$

The radiation conductance is frequency dependent through k_0 . We note that there is an implicit k_0 dependence through the Fourier transforms of the aperture modes, and we set $|\mathbf{k}| = k_0$ in (6) and (8). The remaining part of (4) gives the radiation

susceptance. Part of this can be expressed as a principle part integral of the radiation conductance. However, there is an additional inductive contribution ($Y \propto k_0^{-1}$) (which we term the magnetostatic conductance) coming from the last term in the parentheses in (5) that contains a factor that cancels the resonant denominator in (4). The reactive response of the aperture can be expressed in terms of the Cauchy principal value of the radiation conductance (4), and the previously mentioned inductive contribution, yielding

$$B_{ss'}^{\text{rad}}(k_0) = P \int_0^\infty \frac{2k_0 dk}{\pi(k_0^2 - k^2)} G_{ss'}^{\text{rad}}(k) + B_{ss'}^{m,s} \quad (9)$$

where $B_{ss'}^{m,s}$ stands for magnetostatic conductance, defined as

$$B_{ss'}^{m,s}(k_0) = \frac{2}{k_0} \sqrt{\frac{\epsilon}{\mu}} \int \frac{dk^3}{(2\pi)^3} \tilde{\mathbf{e}}_s^* \cdot \underline{\Delta}_{B^{ms}} \cdot \tilde{\mathbf{e}}_{s'} \quad (10)$$

and where $\underline{\Delta}_{B^{ms}} = [(\mathbf{k} \times \hat{n})(\mathbf{k} \times \hat{n})]/k^2$.

We now repeat the process, but assume that the aperture opens into a cavity rather than an infinite half-space, the radiation admittance (4) will be replaced by a cavity admittance. In the appendix, it is shown that under the assumptions that the eigenmodes of the closed cavity can be replaced by superpositions of random plane waves (Berry's hypothesis [29], [30]), and the spectrum of the cavity eigenmodes can be replaced by one corresponding to a random matrix from the Gaussian Orthogonal Ensemble (GOE) [22], the statistical properties of the cavity admittance can be represented as

$$\underline{Y}^{cav} = i\underline{B}^{\text{rad}} + \left[\underline{G}^{\text{rad}} \right]^{1/2} \cdot \underline{\xi} \cdot \left[\underline{G}^{\text{rad}} \right]^{1/2} \quad (11)$$

and the matrix $\underline{\xi}$ is a universal fluctuation matrix defined as

$$\underline{\xi} = \frac{i}{\pi} \sum_n \frac{\Phi_n \Phi_n^T}{\mathcal{K}_0 - \mathcal{K}_n + i\alpha} \quad (12)$$

where \mathcal{K}_n is a set of eigenvalues of a random matrix drawn from the GOE [22]. These matrices have positive and negative eigenvalues that fall in a symmetric range about zero. The mean spacing of the eigenvalues near zero can be adjusted by scaling the size of the matrix elements. Here we assume that this has been done such that the mean spacing of the \mathcal{K}_n near zero is unity. The quantity \mathcal{K}_0 represents the deviation of the excitation frequency ω_0 from some reference value ω_{ref} placed in the band of interest

$$\mathcal{K}_0 = \frac{\omega_0 - \omega_{\text{ref}}}{\Delta\omega} \quad (13)$$

where $\Delta\omega$ is the mean spacing between the resonant frequencies of modes of the actual cavity in the range of ω_{ref} . The resonant frequencies of a particular realization are, thus, given by $\omega_n = \omega_{\text{ref}} + \Delta\omega \mathcal{K}_n$. The vector Φ_n is composed of independent, zero mean, unit variance Gaussian random variables. The quantity α describes the average loss in the cavity and is related to the finesse parameter \mathcal{F} , widely used in optical cavities and photonic lattices [31]

$$\alpha = \mathcal{F}^{-1} = \frac{\omega_0}{2Q\Delta\omega} \quad (14)$$

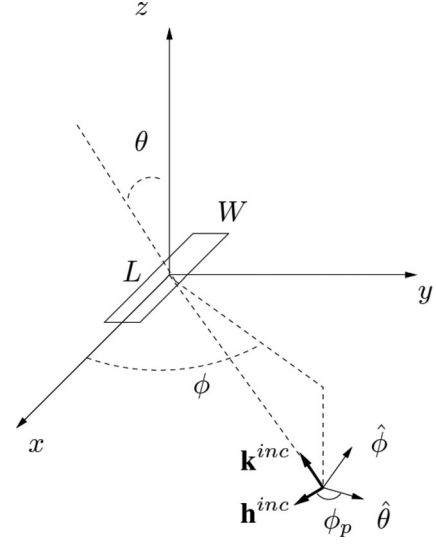


Fig. 2. Geometry of a 2-D regular (narrow) aperture illuminated by an external plane wave, radiating in free space.

Thus, according to the RCM, two quantities are required to specify the properties of the cavity: the Q width ω_0/Q and the mean spacing $\Delta\omega$ between nearest neighbor resonances (cavity modes).

The quantity α determines whether the cavity is in the high-loss ($\alpha > 1$) or low-loss ($\alpha < 1$) regime. More precisely, it establishes how much the individual resonances overlap. Basically, if $\alpha > 1$ the Q -width of a resonance ω_0/Q exceeds the spacing between resonances $\Delta\omega$. A feature of chaotic cavities is that each mode in a given frequency band has essentially the same Q width. This is a consequence of the ergodic nature of the ray trajectories that underlie the mode structure. Each mode has wave energy distributed throughout the cavity such that losses are approximately the same for each mode.

We now describe how relations (3) and (11) are used to determine the coupling of our system to external radiation. Specifically, we consider the framework of Fig. 2, where the aperture is illuminated by a plane wave incident with a wave vector \mathbf{k}^{inc} and polarization of magnetic field \mathbf{h}^{inc} that is perpendicular to \mathbf{k}^{inc} . We again consider the aperture to be an opening in a conducting plane at $z = 0$, with radiation incident from $z = -\infty$. We imagine writing the fields for $z < 0$ as the sum of the incident wave, the wave that would be specularly reflected from an infinite planar surface, and a set of outgoing waves associated with the presence of the aperture. The incident and specularly reflected waves combine to produce zero tangential electric field on the plane $z = 0$. Thus, the outgoing waves for $z < 0$ associated with the aperture can be expressed in terms of the electric fields in the aperture just as the outgoing waves for $z > 0$ can, the two cases being mirror images. So, relation (1) continues to represent the tangential electric fields in the plane $z = 0$. For the magnetic field, we have separate expansions for $z > 0$ and $z < 0$. The electric field amplitudes are then determined by the condition that the magnetic fields are continuous in the aperture at $z = 0$. For $z = 0+$, we have

$\mathbf{H}_t^> = \sum_s I_s^> \hat{n} \times \mathbf{e}_s(\mathbf{x}_\perp)$, with $\underline{I}^> = \underline{Y}^> \cdot \underline{V}$, where $\underline{Y}^>$ is either the radiation admittance matrix (4) or the cavity admittance matrix (11) depending on the circumstance. For $z = 0^-$, we have $\mathbf{H}_t^< = \sum_s I_s^< \hat{n} \times \mathbf{e}_s(\mathbf{x}_\perp) + 2\mathbf{h}^{\text{inc}} \exp[i\mathbf{k}^{\text{inc}} \cdot \mathbf{x}_\perp]$, where $\underline{I}^< = -\underline{Y}^{\text{rad}} \cdot \underline{V}$ (the minus sign accounts for the mirror symmetry) and the factor of two multiplying the incident field comes from the addition of the incident and specularly reflected magnetic fields. Projecting the two magnetic field expressions on the aperture basis, and equating the amplitudes gives

$$\left(\underline{Y}^> + \underline{Y}^{\text{rad}} \right) \cdot \underline{V} = 2\underline{I}^{\text{inc}} \quad (15)$$

where

$$\underline{I}_s^{\text{inc}} = -\hat{n} \cdot \tilde{\mathbf{e}}_s(-\mathbf{k}_\perp^{\text{inc}}) \times \mathbf{h}^{\text{inc}} \quad (16)$$

and $\tilde{\mathbf{e}}_s$ is the Fourier transform of the aperture electric field and is defined in (6). Equation (15) can be inverted to find the vector of voltages

$$\underline{V} = \left(\underline{Y}^{\text{rad}} + \underline{Y}^> \right)^{-1} \cdot 2\underline{I}^{\text{inc}} \quad (17)$$

and then the net power passing through the aperture is given by

$$P_t = \frac{1}{2} \Re \left(\underline{V}^* \cdot \underline{Y}^> \cdot \underline{V} \right) \quad (18)$$

where $\underline{Y}^>$ can be either a radiation (free-space) admittance (4) or a cavity admittance matrix (11).

III. RECTANGULAR APERTURES

We consider rectangular apertures and select a basis for representation of the tangential fields in the aperture in (1) and (2). One choice for the basis is the modes of a waveguide with a rectangular cross section. These can be written either as a sum of TE and TM modes, or simply as a Fourier representation of the individual Cartesian field components [32], [33].

In EMC studies, narrow apertures are often considered, as they frequently occur in practical EM scenarios. The aperture of Fig. 2 is elongated and thin: it has only one electrically large dimension, and the field component $\mathbf{e}_{(n,0)}(x) \approx 0$, with $s = (n, 0)$. Hence, in the particular case of a rectangular aperture with $L \sim \lambda \gg W$ and $W \rightarrow 0$, the field will be dominated by TE_{n0} modes

$$\mathbf{e}_s \approx \frac{\sin[k_n(x + L/2)]}{N} \hat{y} \quad (19)$$

for $|y| < W/2$, where $N = \sqrt{2/LW}$. Once the aperture field basis is specified, the procedure for calculating the cavity admittance matrix (4) is given by the following steps [34]: first, calculate the Fourier transform $\tilde{\mathbf{e}}_s$ (6); second, use $\tilde{\mathbf{e}}_s$ to calculate the radiation conductance (7); third, use $\tilde{\mathbf{e}}_s$ to calculate the magnetostatic susceptance (10); and fourth, use the aforesaid quantities to form the radiation susceptance $G_{ss}^{\text{rad}} + iB_{ss}^{\text{rad}}$. Finally, use the so-formed radiation admittance to generate the cavity admittance (11), similar to [6], [35]. The conductance and susceptance have the property that off-diagonal terms vanish if n is odd and n' is even, and vice versa, due to the even and

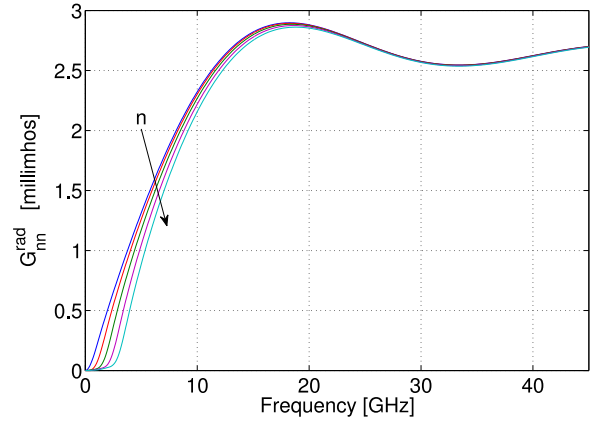


Fig. 3. Diagonal radiation conductance for $n = 1, \dots, 5$, for a narrow aperture $L = 25 \text{ cm} \times W = 2 \text{ cm}$. In the inset: low-frequency (cutoff) detail of the diagonal elements with an off-diagonal element.

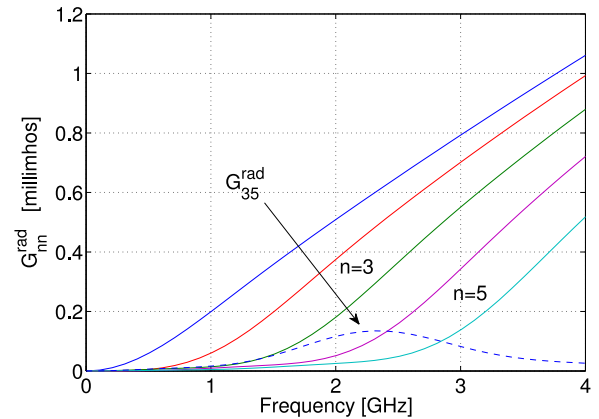


Fig. 4. Closeup of the diagonal radiation conductance in Fig. 3: low-frequency (cutoff) detail of the diagonal elements with an off-diagonal element (dashed line). The mode index n increases from left to right as indicated in Fig. 3.

odd parity in x of the basis modes. Further, in the limit of high frequency, $k_0 \gg k_n$, the components $G_{nn'}$ have the limits

$$G_{nn'}^{\text{rad}} \rightarrow \begin{cases} \sqrt{\frac{\epsilon}{\mu}} & n = n' \\ 0 & n \neq n' \end{cases} \quad (20)$$

Thus, at high frequencies the admittance matrix $\underline{Y}_{ss'}^{\text{rad}}$ is diagonal and equal to the free-space conductance as would be expected when the radiation wavelength is much smaller than the aperture size.

We have evaluated the elements of the radiation conductance matrix as functions of frequency for a rectangular aperture with dimensions $L = 25 \text{ cm} \times W = 2 \text{ cm}$. Plots of these appear in Figs. 3 and 4. For the diagonal elements, the conductance increases nonmonotonically from zero, and asymptotes to its free-space value. For the off-diagonal components (not shown), the conductance first rises and then falls to zero with increasing frequency. Combining numerical evaluations of the two contributions in (9) yields the total susceptance. This is plotted for several diagonal elements in Fig. 5, which have the feature that for some elements the susceptance passes through zero at

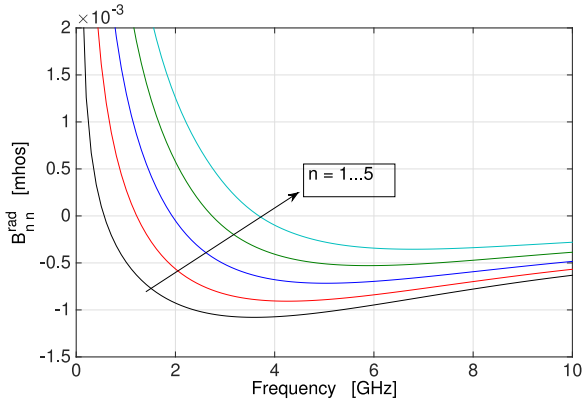


Fig. 5. Diagonal radiation susceptance for $n = 1, \dots, 5$, for a narrow aperture $L = 25 \text{ cm} \times W = 2 \text{ cm}$.

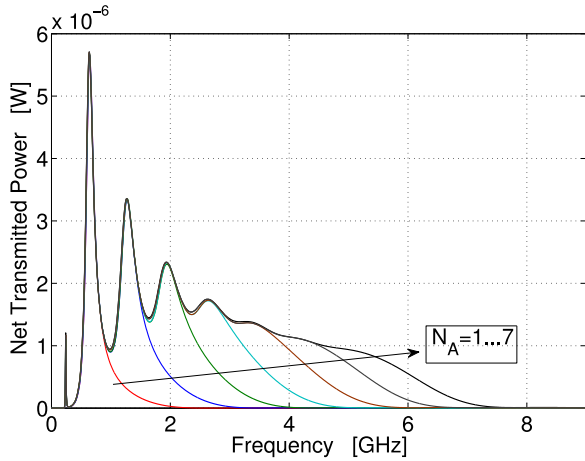


Fig. 6. Frequency behavior of the net power transmitted by an aperture $\mathcal{A} = 0.25 \text{ m} \times 0.02 \text{ m}$ in free space, $N_{\mathcal{A}} = 1, \dots, 7$ modes, for an external plane wave of $h^{\text{inc}} = 1 \text{ mA/m}$, at oblique incidence $\phi = 0$, $\theta = \pi/4$, and polarization $\phi_p = \pi/2$.

a particular frequency. At these frequencies, the conductances (see Fig. 4) also tend to be small. This indicates the presence of resonant modes of the aperture. At the frequencies of these modes, the aperture will allow more power to pass through the plane of the conductor than would be expected based on the aperture area. Our next step is to evaluate the power passing through the aperture when it is illuminated by a plane wave. This involves solving (17) for the vector of voltages \underline{V} , and inserting these in (18) for the power transmitted through the aperture. This will be done a number of times; first with $\underline{Y}^> = \underline{Y}^{\text{rad}}$ to determine the power passing through the aperture in the radiation case; then again with $\underline{Y}^> = \underline{Y}^{\text{cav}}$ to determine the power through the aperture when it is backed by a cavity. In the cavity case, a number of realizations of the cavity admittance matrix will be considered, modeling cavities with different distributions of resonant modes.

Fig. 6 shows the frequency behavior of the transmitted power defined in (18), with $\underline{Y}^> = \underline{Y}^{\text{rad}}$, for an oblique plane wave

incident with angles $\phi_p = \pi/2$, $\phi = 0$, and $\theta = \pi/4$, according to the coordinate frame of Fig. 2. In Fig. 6, the net power is parameterized by the number of aperture modes included in the calculation, ranging from $N_{\mathcal{A}} = 1$ to $N_{\mathcal{A}} = 7$. As expected, the higher the frequency the greater the number of modes required to achieve an accurate prediction of the transmitted power. Interestingly, we notice the presence of a sharp peak at 600 MHz, which is the slit resonance frequency, i.e., $f_A = c/(2L)$, and other broader resonances located at $n f_A$. At normal incidence, the peak of the resonance next to the sharp peak is reduced of a factor of 10. This is confirmed in previous studies based on the transmission line model of a narrow aperture [36]. Having computed the radiation conductance and susceptance for a narrow slit of dimensions $25 \text{ cm} \times 2 \text{ cm}$, we can investigate the effect of a wave-chaotic cavity backing the aperture by replacing $\underline{Y}^{\text{rad}}$ by $\underline{Y}^{\text{cav}}$ and exploiting the statistical model, (11). We first calculate distributions of the cavity admittance elements from the RCM by using a Monte Carlo technique and the radiation admittance of a rectangular aperture. Numerical calculations of (4) and Monte Carlo simulation of (12) allow for generating an ensemble of cavity admittances of the form (11). In particular, we use the statistical method described in [5] and [6], with $N = 7$ aperture modes, $M = 600$ cavity modes, and a loss factor of $\alpha = 6$, simulating a chaotic cavity with high losses, to create the bare fluctuation matrix (12). Here, we repeat the simulation of (12) 800 times to create an ensemble of fluctuation matrices. By virtue of its construction, the average cavity admittance equals the radiation matrix $\langle \underline{Y}^{\text{cav}} \rangle = \underline{Y}^{\text{rad}}$. Further, in the high-loss limit ($\alpha \gg 1$) fluctuations in the cavity matrix become small and $\underline{Y}^{\text{cav}} \rightarrow \underline{Y}^{\text{rad}}$. For finite losses, the character of the fluctuations in the elements of the cavity admittance matrix changes from Lorentzian at low loss ($\alpha \ll 1$) to Gaussian at high loss ($\alpha \gg 1$).

We now consider the net power coupled through an aperture that is backed by a wave-chaotic cavity. This involves evaluating (17) and (18) with $\underline{Y}^> = \underline{Y}^{\text{cav}}$ and with $\underline{Y}^{\text{cav}}$ evaluated according to (11). When this is done, the frequency dependence of the net power acquires structure that is dependent on the density of modes in the cavity. This is illustrated in Figs. 7 and 8, where net power through the 0.25 m by 0.02 m rectangular aperture is plotted versus frequency in the range $1.0 < f < 1.2 \text{ GHz}$ for a few realizations of the fluctuating admittance matrix. In both cases, the reference frequency in (13) is set at $f_{\text{ref}} = \omega_{\text{ref}}/(2\pi) = 1.1 \text{ GHz}$, and the mean spacing between modes is set to be $\Delta f = \Delta\omega/(2\pi) = 10 \text{ MHz}$. Fig. 7 corresponds to a moderate loss case ($\alpha = 1.0$), and Fig. 8 to a low-loss case ($\alpha = 0.1$). Clearly, in the low-loss case the peaks in power associated with different resonances are more distinct and extend to higher power. Also, plotted in Figs. 7 and 8 are the average over 800 realizations of the power coupled into the cavity and the power coupled through the aperture in the radiation case. Notice that both of these curves are smooth functions of frequency and that in the moderate loss case of Fig. 7 the power averaged over many realizations $\langle P_{\text{cav}} \rangle$ is only slightly less than the transmitted power in the radiation case. In the low-loss

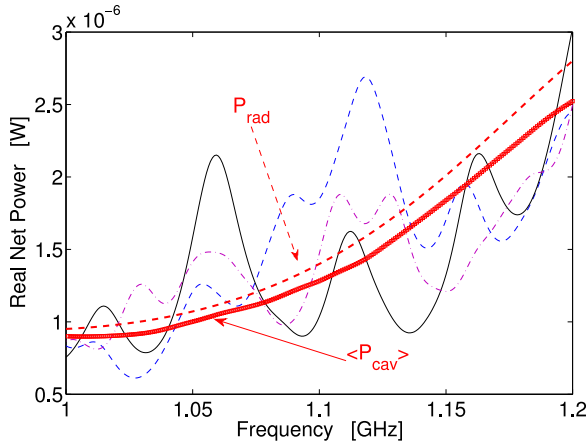


Fig. 7. Comparison between the radiation (red dashed line), and the average (red squares) net power transmitted by an aperture of dimensions $\mathcal{A} = 0.25 \text{ m} \times 0.02 \text{ m}$, in the frequency range from 1 to 1.2 GHz for an external incidence of $h^{\text{inc}} = 1 \text{ A/m}$, direction of incidence $\phi = 0$, $\theta = \pi/4$, polarization $\phi_p = \pi/2$. Thin solid (black), dashed (blue), and dash-dotted (purple) lines are reported to show three independent cavity realizations as generated through a Monte Carlo method. The thick solid (red) line indicates the ensemble average of the port power over 800 cavity realizations. The thick dashed (red) line indicates the power radiated from the aperture in free space. Each cavity response is given by the superposition of 600 ergodic eigenmodes. The chaotic cavity is modeled with $\alpha = 1.0$.

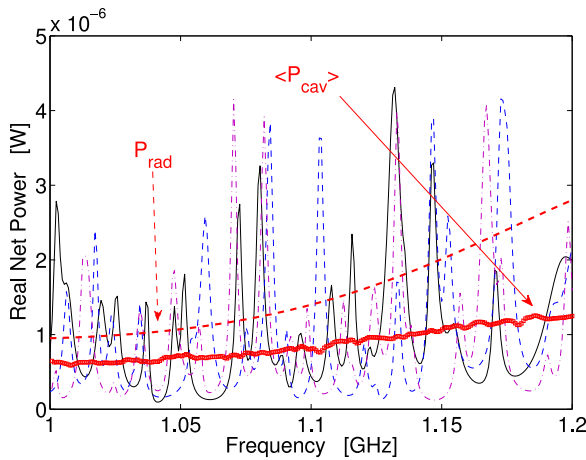


Fig. 8. Comparison between the radiation (red dashed line), and the average (red squares) net power transmitted by an aperture of dimensions $\mathcal{A} = 0.25 \text{ m} \times 0.02 \text{ m}$, in the frequency range from 1 to 1.2 GHz for an external incidence of $h^{\text{inc}} = 1 \text{ A/m}$, direction of incidence $\phi = 0$, $\theta = \pi/4$, polarization $\phi_p = \pi/2$. Thin solid (black), dashed (blue), and dash-dotted (purple) lines are reported to show three independent cavity realizations as generated through a Monte Carlo method. The thick solid (red) line indicates the ensemble average of the port power over 800 cavity realizations. The thick dashed (red) line indicates the power radiated from the aperture in free space. Each cavity response is given by the superposition of 600 ergodic eigenmodes. The chaotic cavity is modeled with $\alpha = 0.1$.

case of Fig. 8, the average power coupled into the cavity is about half the value of the radiation case.

The features of the coupled power in Figs. 7 and 8 can be captured by a simple model. We consider the frequency range in Fig. 6, where the resonances in the aperture are isolated, roughly speaking $f < 3 \text{ GHz}$. In this case, in a given narrow frequency range the aperture fields are dominated by a single

mode, and we can replace the matrix (15)–(18) with their scalar versions, yielding

$$P_t = 2 |I^{\text{inc}}|^2 \Re \left\{ \frac{Y^>}{|Y^{\text{rad}} + Y^>|^2} \right\} \quad (21)$$

where $Y^> = Y^{\text{rad}}$ or Y^{cav} depending on whether a cavity is present, $Y^{\text{rad}} = iB^{\text{rad}} + G^{\text{rad}}$ and $Y^{\text{cav}} = iB^{\text{rad}} + G^{\text{rad}}\xi$ with

$$\xi = \frac{i}{\pi} \sum_{n'} \frac{w_{n'}^2}{\mathcal{K}_0 - \mathcal{K}_{n'} + i\alpha}. \quad (22)$$

Here, \mathcal{K}_0 , $\mathcal{K}_{n'}$, and α are defined as before following (12) and the $w_{n'}$ is a set of independent and identically distributed Gaussian random variables with zero mean and unit variance. The quantities B^{rad} and G^{rad} are properties of the aperture, and will be discussed later.

The power transmitted through the aperture in the absence of a cavity is given by

$$P_t = \frac{|I^{\text{inc}}|^2}{2} \frac{G^{\text{rad}}}{|G^{\text{rad}} + iB^{\text{rad}}|^2}. \quad (23)$$

The aperture resonance occurs at a frequency ω_A , where $B^{\text{rad}}(\omega_A) = 0$, corresponding to a peak in Fig. 6, and the coupled power at the peak is $P_A = P_t(\omega_A) = |I^{\text{inc}}|^2 / (2G^{\text{rad}})$, with $G^{\text{rad}} = G^{\text{rad}}(\omega_A)$. We can then express the frequency dependence of the power coupled through the aperture for frequencies near ω_A in the form of a Lorentzian resonance function

$$P_t(\omega) = \frac{P_A}{1 + \Delta_A^2} \quad (24)$$

where

$$\Delta_A = \frac{2Q_A(\omega - \omega_A)}{\omega_A} \quad (25)$$

and the effective quality factor for the aperture is given by

$$Q_A = \frac{\omega_A}{2G^{\text{rad}}(\omega_A)} \left. \frac{dB^{\text{rad}}}{d\omega} \right|_{\omega_A}. \quad (26)$$

When a cavity backs the aperture, $Y^> = Y^{\text{cav}}$ becomes a random frequency-dependent function through the variable $\xi(\omega)$. This quantity is frequency dependent through the denominators in (22) and is random due to the random vectors of coupling coefficients w_n and eigenvalues \mathcal{K}_n . The frequency scale for variation of $\xi(\omega)$ is determined by the frequency spacing of modes of the cavity. In the typical case, the frequency spacing of cavity modes is much smaller than that of aperture modes, as depicted in Figs. 7 and 8. The behavior of the coupled power as a function of frequency will, thus, follow the envelope of the radiation case, with fluctuations on the frequency scale of the separation between cavity modes.

This behavior can be captured in the simple mode if we assume the frequency is close to one of the poles ($n' = n$) of (22). Specifically, we write

$$\xi = ib + \frac{iw_n^2}{\pi(\mathcal{K}_0 - \mathcal{K}_n + i\alpha)} \quad (27)$$

where the term ib is in the form of (22) with the $n' = n$ term removed and $\mathcal{K}_0 = \mathcal{K}_n$. Since α is assumed to be small it can

be neglected in b (making b purely real), whereas it is retained in the second term in (27) since we consider frequencies such that $\mathcal{K}_0 - \mathcal{K}_n$ is small and comparable to α . The statistical properties of the sum given by b were detailed by Hart *et al.* [37]. If we express b in the form $b = \tan \psi$, then the PDF of ψ is $\cos \psi/2$ [37]. For now, since we are focusing on the behavior of individual realizations, we leave the value of b unspecified.

Having assumed the cavity response is dominated by a single resonance, we can manipulate (21) into a general form

$$P_t(\omega) = P_A \frac{4\alpha\alpha_A}{|\mathcal{K}_0 - \mathcal{K}'_n + i(\alpha + \alpha_A)|^2} \quad (28)$$

where $\mathcal{K}'_n = \mathcal{K}_n - 2\Delta'\alpha_A$, $\Delta' = \Delta_A + b/2$, and

$$\alpha_A = \frac{w_n^2}{\pi |1 + 2i\Delta'|^2}. \quad (29)$$

Here, the variables have the following interpretations: α_A is the “external” loss factor describing the damping of the cavity mode due to the aperture. Note, it is added to the internal loss factor α in the denominator of (28). It is a statistical quantity, mainly through the Gaussian random variables w_n . This is responsible for variation in the height of the peaks in Fig. 8. The quantity $\Delta' = \Delta_A + b/2$ represents the modification of the aperture resonance function (25) by the reactive fields of the nonresonant cavity modes ($b/2$). Note that it affects the external damping factor α_A , which is largest when $\Delta' = 0$, i.e., when ω is near the aperture resonant frequency. Finally, \mathcal{K}'_n determines the shifted cavity mode frequency. That is, using definition (13) the resonant cavity mode frequency, $\mathcal{K}_0 = \mathcal{K}'_n$, becomes

$$\omega = \omega_n - 2\Delta\omega\Delta'\alpha_A. \quad (30)$$

Equation (28) implies that the power coupled into the cavity at frequency ω is bounded above by the power that can be transmitted through the aperture at the aperture resonance ω_A . These powers are equal $P_t(\omega) = P_A$ if the mode is resonant, $\mathcal{K}_0 = \mathcal{K}'_n$, and the cavity is critically coupled, $\alpha = \alpha_A$. Note, however, that the coupled power in the cavity case (28) can exceed the radiation case (24) at the same frequencies if the aperture is off resonance $\Delta'(\omega) \neq 0$. This is evident at the peaks of the coupled power in Fig. 8. Basically, what is happening is the cavity susceptance, which alternates in sign as frequency varies on the scale of the cavity modes, cancels the aperture susceptance, thus making the aperture resonant for frequencies away from the natural resonance ω_A .

When the cavity loss parameter is small as in Fig. 8 or (28) there are large variations in coupled power as frequency is varied. A broad band signal would average over these variations. We can treat this case by computing the power coupled through the aperture averaged over realizations of the random variable ξ defined in (22). Such averages are shown in Figs. 7 and 8 based on Monte Carlo evaluations of the full system (18). We perform this average in our simple model. A plot of a numerical evaluation of $\langle P_t \rangle / P_A$ from (28) as a function of Δ' for different loss parameters α appears in Fig. 9. Interestingly, a loss parameter that is as large as $\alpha = 1$ is sufficient to make the average power entering a cavity 90% of that passing through an unbacked aperture.

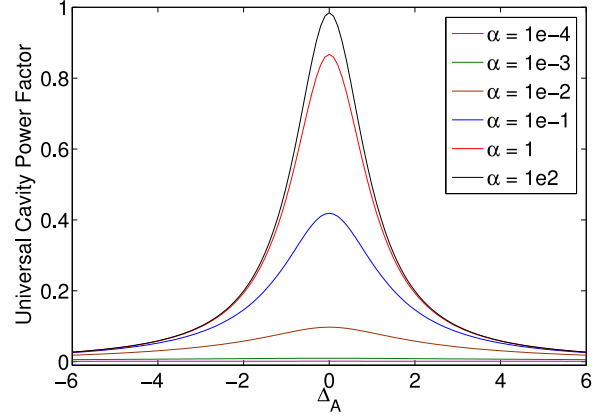


Fig. 9. Universal aperture factor on Δ_A , parameterized by α .

IV. CAVITY WITH BOTH PORTS AND APERTURES

In the previous section, we determined the properties of the power entering a cavity through an aperture. The contents of the cavity were treated as a distributed loss characterized by a single parameter α . We will now extend this model to treat the case in which we identify a second port to the cavity that we will treat as an electrically small antenna. This port could be an actual port, where a connection is made to the outside world as illustrated in Fig. 1, or the port could represent the pin of a circuit element on which the voltage is of interest.

We consider the configuration of Fig. 1, where we have the joint presence of apertures and ports. We have previously considered the case of fields excited by a current distribution of the form [38]

$$\mathbf{J}(\mathbf{x}) = \sum_p \mathbf{u}_p(\mathbf{x}) I_p, \quad (31)$$

where $\mathbf{u}_p(\mathbf{x})$ is a set of basis functions used to represent the current distribution in terms of a set of amplitudes I_p , which we call the port currents. The corresponding port voltages were defined in [38] as

$$V_p = - \int d^3x \mathbf{u}_p(\mathbf{x}) \cdot \mathbf{E}(\mathbf{x}) \quad (32)$$

and as a result the power entering the cavity through the ports is $P_p = \Re \left\{ \sum_p V_p^* I_p \right\} / 2$.

In analogy to our treatment of the aperture, we consider two cases: one in which the current distribution radiates into free space and one in which the current distribution radiates into a cavity. The linear relationship between the port voltages V_p and the port currents I_p is then characterized by impedance matrices $Z_{pp'}^{\text{rad}}$ and $Z_{pp'}^{\text{cav}}$ depending on the case under consideration, where

$$V_p = \sum_{p'} Z_{pp'}^{\text{rad/cav}} I_{p'}. \quad (33)$$

For the radiation case, it was shown [38]

$$Z_{pp'}^{\text{rad}}(k_0 = \omega/c) = \sqrt{\frac{\mu}{\epsilon}} \int \frac{d^3k}{(2\pi)^3} \frac{ik_0}{k_0^2 - k^2} \tilde{\mathbf{u}}_p \cdot \tilde{\mathbf{u}}_{p'}^* \quad (34)$$

where $\tilde{\mathbf{u}}_p(k)$ is the Fourier transform of the basis function $\mathbf{u}_p(\mathbf{x})$, $k_0 = \omega/c$, and the dyadic $\underline{\Delta}_Z$ is given by

$$\underline{\Delta}_Z = \frac{\mathbf{1}k^2 - \mathbf{k}\mathbf{k}}{k^2} + \frac{\mathbf{k}\mathbf{k}}{k^2 k_0^2} (k_0^2 - k^2). \quad (35)$$

The radiation impedance matrix can be decomposed $Z_{pp'}^{\text{rad}} = R_{pp'}^{\text{rad}} + iX_{pp'}^{\text{rad}}$, where $R_{pp'}^{\text{rad}}$ is the residue from the pole at $k = k_0$ in (34) (the radiation resistance)

$$R_{pp'}^{\text{rad}}(k_0) = \Re\left(Z_{pp'}^{\text{rad}}\right) = \sqrt{\frac{\mu}{\epsilon}} \int \frac{k_0^2 d\Omega_k}{16\pi^2} \tilde{\mathbf{u}}_p^* \cdot \frac{\mathbf{1}k^2 - \mathbf{k}\mathbf{k}}{k^2} \cdot \tilde{\mathbf{u}}_{p'}^* \quad (36)$$

and $X_{pp'}^{\text{rad}}$ is the reactive contribution.

For the cavity case, it was shown

$$\underline{Z}^{\text{cav}} = i\Im\left\{\underline{Z}^{\text{rad}}\right\} + \left[\underline{R}^{\text{rad}}\right]^{1/2} \cdot \underline{\xi} \cdot \left[\underline{R}^{\text{rad}}\right]^{1/2} \quad (37)$$

where the fluctuating matrix $\underline{\xi}$ is defined in (12).

We are now in a position to describe a statistical model for a cavity including both an aperture and a localized current distribution. In this case, we construct an input column vector $\underline{\phi}$ that consists of the aperture voltages and port currents and an output vector $\underline{\psi}$ that consists of the aperture currents and port voltages

$$\underline{\phi} = \begin{bmatrix} \underline{V}_A \\ \underline{I}_P \end{bmatrix} \quad (38)$$

and

$$\underline{\psi} = \begin{bmatrix} \underline{I}_A \\ \underline{V}_P \end{bmatrix} \quad (39)$$

where $\underline{V}_{A,P}$ are the aperture and port voltages, and $\underline{I}_{A,P}$ are the aperture and port currents. These are then related by a hybrid matrix \underline{T} , $\underline{\psi} = \underline{T} \cdot \underline{\phi}$, where

$$\underline{T} = i\text{Im}\left(\underline{U}\right) + \left[\underline{V}\right]^{1/2} \cdot \underline{\xi} \cdot \left[\underline{V}\right]^{1/2}. \quad (40)$$

Here, the matrices \underline{U} and \underline{V} are block diagonal, viz.,

$$\underline{U} = \begin{bmatrix} \underline{Y}^{\text{rad}} & 0 \\ 0 & \underline{Z}^{\text{rad}} \end{bmatrix} \quad (41)$$

and $\underline{V} = \Re\left[\underline{U}\right]$. The dimension of \underline{U} and \underline{V} is $(N_s + N_p) \times (N_s + N_p)$, where N_p is the number of port currents and N_s is the number of aperture voltages. Here, we have assumed that the ports and apertures are sufficiently separated such that the off-diagonal terms in \underline{U} , describing the direct excitation of port voltages by aperture voltages, and aperture currents by port currents, are approximately zero. This assumption can be released in case of direct illumination between, or proximity of, aperture and port through the short-orbit correction of the RCM, which in this setting needs to be extended to cope with vector EM fields [37], [39]. In the simplest case, we can take the square

root of \underline{V}

$$\left[\underline{V}\right]^{1/2} = \begin{bmatrix} \left[\underline{G}^{\text{rad}}\right]^{1/2} & 0 \\ 0 & \left[\underline{R}^{\text{rad}}\right]^{1/2} \end{bmatrix}. \quad (42)$$

At this point, we specialize consideration to the case of a port that is an electrically small antenna characterized by a single current I_p and single basis function in (31). The matrices \underline{T} , \underline{U} , and \underline{V} then have dimension $(N_A + 1) \times (N_A + 1)$ and the matrix relations for the voltages and currents are more clearly expressed when separated into N_A aperture equations and one port equation. For the aperture equations, we find that (15) is replaced by

$$\left(\underline{Y}^{\text{cav}} + \underline{Y}^{\text{rad}}\right) \cdot \underline{V}_A + \left[\underline{G}^{\text{rad}}\right]^{1/2} \cdot \underline{\xi}_{\text{AP}} \cdot \left(R^{\text{rad}}\right)^{1/2} I_p = 2\underline{I}^{\text{inc}}. \quad (43)$$

For the port, we assume the small antenna drives a load with impedance Z_L such that $V_p = -Z_L I_p$. Then, the port equation becomes

$$\left(Z_L + Z^{\text{cav}}\right) I_p + \left(R^{\text{rad}}\right)^{1/2} \underline{\xi}_{\text{AP}}^T \cdot \left[\underline{G}^{\text{rad}}\right]^{1/2} \cdot \underline{V}_A = 0 \quad (44)$$

where $\underline{\xi}_{\text{AP}}$ is a column vector defined similarly to the $N_A \times N_A$ matrix $\underline{\xi}$ in (12). Finally, the scalar cavity impedance is defined in accord with (37)

$$Z^{\text{cav}} = iX^{\text{rad}} + R^{\text{rad}} \xi \quad (45)$$

with ξ being a scalar version of the fluctuation matrix. If we assume the aperture voltages are known, (44) can be solved for the current in the port

$$I_p = -\left(Z_L + Z^{\text{cav}}\right)^{-1} \left(R^{\text{rad}}\right)^{1/2} \underline{\xi}_{\text{AP}}^T \cdot \left[\underline{G}^{\text{rad}}\right]^{1/2} \cdot \underline{V}_A. \quad (46)$$

Substituting the expression for the port current into the aperture (43) yields an equation of the form of (15) for the aperture voltages

$$\left(\underline{Y}^{\text{rad}} + \underline{Y}^{\text{cav}'}\right) \cdot \underline{V}_A = 2\underline{I}^{\text{inc}}. \quad (47)$$

Here, the modified cavity admittance

$$\underline{Y}^{\text{cav}'} = \underline{Y}^{\text{cav}} - \frac{R^{\text{rad}}}{\left(Z_L + Z^{\text{cav}}\right)} \left[\underline{G}^{\text{rad}}\right]^{1/2} \cdot \underline{\xi}_{\text{AP}} \cdot \underline{\xi}_{\text{AP}}^T \cdot \left[\underline{G}^{\text{rad}}\right]^{1/2} \quad (48)$$

includes the effect of the current induced in the port antenna on the magnetic fields at the aperture. In the high-loss limit ($\alpha > 1$) or if the antenna load impedance is large this last term is small, $\underline{Y}^{\text{cav}'} \approx \underline{Y}^{\text{cav}}$, and the amount of power coupled through the aperture is unaffected by the presence of the antenna. Once (47) is inverted to find the aperture voltages \underline{V}_A (48) can be used to find the current induced in the antenna, and the relation $V_p = -Z_L I_p$ can be used to find the port voltage. The power dissipated in the load is then $P_L = R_L |I_p|^2 / 2$.

We first consider the statistical properties of the fluctuating port voltage V_p in the high-loss limit. As mentioned, in this case $\underline{Y}^{\text{cav}'} \approx \underline{Y}^{\text{cav}}$, and further $\underline{Y}^{\text{cav}} \approx \underline{Y}^{\text{rad}}$. Thus, the aperture voltages \underline{V}_A determined by (47) will be the same as those determined in the radiation case of (17) and the power coupled into the cavity will have the character displayed in Fig. 6. Statistical variations in the port current are then determined by the column vector $\underline{\xi}_{\text{AP}}$ in (46). (In the high-loss limit, variations in Z^{cav} become small, and we can replace Z^{cav} with Z^{rad} for the port antenna.)

The statistical properties of the elements of $\underline{\xi}_{\text{AP}}^T$ are the same as those of the off-diagonal elements of the general matrix $\underline{\xi}$ defined in (12). In the limit of high loss, the elements are complex, with independent real and imaginary parts, each of which are zero mean independent Gaussian random variables [5], [6]. The common variance for the real and imaginary parts is $(2\pi\alpha)^{-1}$. Since according to (46) the port current I_p is a linear superposition of Gaussian random variables, it too has independent real and imaginary parts that are zero mean Gaussian random variables. What remains then is to calculate its variance. Specifically, we find

$$\langle |I_p|^2 \rangle = \frac{R^{\text{rad}}}{|Z_L + Z^{\text{rad}}|^2} \frac{1}{\pi\alpha} \underline{V}_A^* \cdot \underline{G}^{\text{rad}} \cdot \underline{V}_A \quad (49)$$

Similar arguments determine the statistics of the port voltage. Since the port voltage and current are complex with independent Gaussian distributed real and imaginary parts, their magnitudes will be Rayleigh distributed with a mean determined by (49). Finally, we calculate the expected power coupled to the load $\langle P_L \rangle = R_L \langle |I_p|^2 \rangle / 2$

$$\langle P_L \rangle = \frac{R_L R^{\text{rad}}}{|Z_L + Z^{\text{rad}}|^2} \frac{1}{2\pi\alpha} P_t \quad (50)$$

where P_t is the power transmitted through the aperture in the radiation case. We note that the ratio of the power coupled to the load and the power entering the cavity satisfies a relation identical to what we found previously for the case of localized ports [40].

The numerical computation of the *exact* expressions (46)–(48) is now carried out. We now describe numerical solutions of the coupled port and aperture (43)–(47). Elements of the matrix $\underline{\xi}$, (12), vector $\underline{\xi}_{\text{AP}}$, and scalar ξ were generated using the same Monte Carlo algorithm used to produce Figs. 7 and 8. Specifically, we generated 800 realizations each with 600 modes. The cavity was excited through a narrow aperture of dimensions $L = 0.25 \text{ m} \times W = 0.02 \text{ m}$, by a plane wave with amplitude $|\mathbf{h}^{\text{inc}}| = 1 \text{ mA/m}$, direction of incidence $\theta = 0$, and $\psi = \pi/2$, with polarization $\phi = \pi/2$, and with frequency swept from 1 to 1.2 GHz. The receiving port was an antenna with free-space impedance $Z^{\text{rad}} = 30 - j20 \Omega$ terminated by a $Z_L = 50 \Omega$ load. Figs. 10 and 11 show the power coupled to the load for the case of loss factor $\alpha = 1.0$ and $\alpha = 0.1$, respectively. As in the cases of the power coupled into the cavity, Figs. 7 and 8, the power to the load for individual realizations shows variations with frequency, which are more pronounced in the low-loss case than in the moderate loss case. Figs. 10 and 11 also display

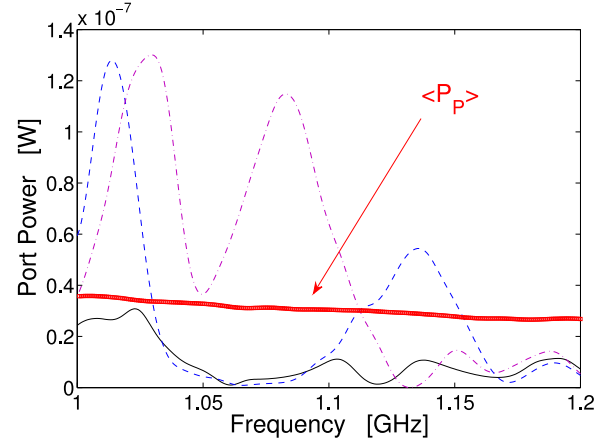


Fig. 10. Port power received by an antenna in the frequency range from 1 to 1.2 GHz. The cavity is highly irregular and overmoded, with loss factor of $\alpha = 1.0$. The aperture is of dimensions $L = 0.25 \text{ m} \times W = 0.02 \text{ m}$, and the external plane wave we assumed has amplitude $|\mathbf{h}^{\text{inc}}| = 1 \text{ mA/m}$, and direction of incidence $\theta = \pi/4$, $\psi = 0$, and $\phi = 0$. Thin solid (black), dashed (blue), and dash-dotted (purple) lines indicate the port power for three independent cavity realizations, while the thick solid (red) line indicates the ensemble average of the port power over 800 cavity realizations. Each cavity response is given by the superposition of 600 ergodic eigenmodes.

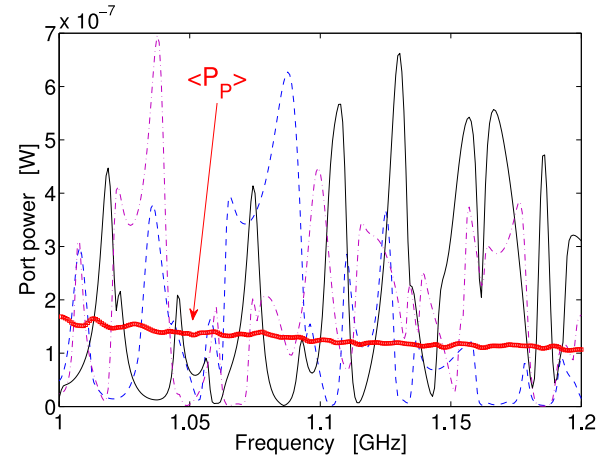


Fig. 11. Port power received by an antenna in the frequency range from 1 to 1.2 GHz. The cavity is highly irregular and overmoded, with loss factor of $\alpha = 0.1$. The aperture is of dimensions $L = 0.25 \text{ m} \times W = 0.02 \text{ m}$, and the external plane wave we assumed has amplitude $|\mathbf{h}^{\text{inc}}| = 1 \text{ mA/m}$, and direction of incidence $\theta = \pi/4$, $\psi = 0$, and $\phi = 0$. Thin solid (black), dashed (blue), and dash-dotted (purple) lines indicate the port power for three independent cavity realizations, while the thick solid (red) line indicates the ensemble average of the port power over 800 cavity realizations. Each cavity response is given by the superposition of 600 ergodic eigenmodes.

the power to the load averaged over the 800 realizations. The amount of power reaching the load is generally in agreement with (50). From Figs. 7 and 8, we see that the average power entering the cavity at 1.1 GHz is 1.6×10^{-6} and $0.6 \times 10^{-6} \text{ W}$ in the $\alpha = 1.0$ and $\alpha = 0.1$ cases, respectively. Equation (50) then predicts for the power reaching the load 0.5×10^{-7} and $2.1 \times 10^{-7} \text{ W}$ in these cases. Note that more power enters the cavity in the higher loss case, but more power reaches the load in the lower loss case. In the low-loss limit, we can develop a formula analogous to (28). We assume the elements of the $\underline{\xi}$ matrix are dominated by a single cavity mode, and make the

same approximations as the one leading to (28). The results for the power coupled to the load is found to be

$$P_L(\omega) = P_A \frac{4\alpha_A \alpha_P}{|\mathcal{K}_0 - \mathcal{K}_n'' + i(\alpha + \alpha_A + \alpha_P)|^2} \quad (51)$$

where P_A is the power coupled through the aperture at resonance, α_A is the aperture loss factor defined in (29), α_P is an analogously defined loss factor for the port

$$\alpha_P = \frac{R_L R^{\text{rad}} w_P^2}{\pi |Z_L + i(X^{\text{rad}} + R^{\text{rad}} b_P)|^2} \quad (52)$$

and $\mathcal{K}_0 = \mathcal{K}_n''$ determines the shifted resonant frequency of mode- n , where

$$\mathcal{K}_n'' = \mathcal{K}_n - 2\delta' \alpha_A - \alpha_P (X^{\text{rad}} + X_L + R^{\text{rad}} b_P) / R_L. \quad (53)$$

In (51), the statistically fluctuating quantities α_P and α_A determine the peak power at resonance reaching the antenna. In the low-loss case considered here, the peak power delivered to the load can be a substantial fraction of the power passing through the aperture at the aperture resonance, P_A .

V. CONCLUSION

We have developed a statistical model of the coupling of EM power through an aperture into a wave chaotic cavity. The formulation combines the deterministic, and system specific elements of the aperture and a receiving antenna in the cavity, with a statistical model for the modes of the cavity. Particular attention has been focused on the case of a rectangular aperture, which has a set of well-separated resonances. Power coupled through an aperture into free space has peaks at frequencies corresponding to the modes of the aperture. When the aperture is backed by a cavity a new set of peaks appears at frequencies of modes of the cavity. These peaks can be as large as the free-space aperture resonance peaks. Simple formulas are derived that augment the detailed formulation, and that apply in the high-loss, low-loss, isolated resonance limit. These results are of interest for studying the coupling of an external radiation through apertures in complex cavities, such as *RCs*, and for practical scenarios of slotted enclosures populated by materials and electronic circuitry.

APPENDIX

The admittance of a cavity excited through an aperture can be expressed by expanding the fields inside the cavity in a basis of electric and magnetic modes

$$\mathbf{E} = \sum_n V_n^{\text{em}} \mathbf{e}_n^{\text{em}}(\mathbf{x}) \quad (54)$$

and

$$\mathbf{H} = \sum_n (I_n^{\text{em}} \mathbf{h}_n^{\text{em}}(\mathbf{x}) + I_n^{\text{ms}} \mathbf{h}_n^{\text{ms}}(\mathbf{x})) \quad (55)$$

Here, the EM modes satisfy the pair of equations, $-ik_n \mathbf{e}_n^{\text{em}} = \nabla \times \mathbf{h}_n^{\text{em}}$, and $ik_n \mathbf{h}_n^{\text{em}} = \nabla \times \mathbf{e}_n^{\text{em}}$ with the tangential components of the electric field equal to zero on the cavity boundary including the aperture. The magnetostatic modes are irrotational

$\mathbf{h}_n^{\text{ms}} = -\nabla \chi_n$, where the potential satisfies the Helmholtz equation $(\nabla^2 + k_n^2) \chi_n = 0$, with Neumann boundary conditions, $|\hat{n} \cdot \nabla \chi_n|_B = 0$. The magnetostatic modes are needed to represent magnetic fields that have nonvanishing normal components at the aperture [41]. It can be shown that all the magnetic field modes are orthogonal.

The mode amplitudes are determined by projecting Maxwell's equations onto the basis functions for each field type. The result of this action is an expression for the magnetic field amplitudes in the aperture that is equivalent to (3) except that the radiation admittance matrix is replaced by a cavity admittance matrix

$$Y_{ss'}^{\text{cav}}(k_0) = \sqrt{\frac{\epsilon}{\mu}} \sum_n \left(\frac{ik_0}{k_0^2 - k_n^2} \frac{w_{sn}^{\text{em}} w_{s'n}^{\text{em}}}{V^{\text{em}}} + \frac{i}{k_0} \frac{w_{sn}^{\text{ms}} w_{s'n}^{\text{ms}}}{V^{\text{ms}}} \right) \quad (56)$$

where

$$w_{sn}^{(\cdot)} = \int_{\text{aperture}} d\mathbf{x}_\perp \mathbf{e}_s(\mathbf{x}_\perp) \cdot \hat{z} \times \mathbf{h}_n^{(\cdot)} \quad (57)$$

is the projection of the magnetic field of the cavity mode onto the aperture field profile and

$$V^{(\cdot)} = \int d\mathbf{x} |\mathbf{h}_n^{(\cdot)}|^2 \quad (58)$$

is a normalization factor for the eigenfunctions.

Expression (56) is general and gives an exact expression for the admittance matrix of a lossless cavity in terms of the cavity modes. If we apply the random coupling hypothesis, we replace the exact eigenmodes with modes corresponding to random superpositions of plane waves. Specifically, near the plane $z = 0$ we write for the components of the EM eigenmodes transverse to the z direction

$$\mathbf{h}_{n\perp}^{\text{em}} = \lim_{N \rightarrow \infty} \frac{2}{\sqrt{N}} \sum_{j=1}^N \mathbf{b}_{j\perp} \cos(\mathbf{k}_j \cdot \hat{n} z) \cos(\theta_j + \mathbf{k}_j \cdot \mathbf{x}_\perp) \quad (59)$$

where θ_j are uniformly distributed in the interval $[0, 2\pi]$, $|\mathbf{k}_j| = k_n$, with the direction of \mathbf{k}_j uniformly distributed over the half solid angle corresponding to $\mathbf{k}_j \cdot \hat{n} > 0$, $|\mathbf{b}_j| = 1$, with \mathbf{b}_j uniformly distributed in angle in the plane perpendicular to \mathbf{k}_j . Except as mentioned, all random variables characterizing each plane wave are independent. A similar expression can be made for the scalar potential χ_n generating the magnetostatic modes. With eigenfunctions expressed as a superposition of random plane waves, each factor $w_{sn^{(\cdot)}}$ appearing in (56) becomes a zero mean Gaussian random variable. The correlation matrix between two such factors can then be evaluated by forming the product of two terms, averaging over the random variables parameterizing the eigenfunctions and taking the limit $N \rightarrow \infty$. We find for the EM modes the following expectation value:

$$\left\langle \frac{w_{sn}^{(\text{em})} w_{s'n}^{(\text{em})}}{V^{\text{em}}} \right\rangle = \int \frac{d\Omega_k}{4\pi V} \tilde{\mathbf{e}}_s^* \cdot \left[\frac{\mathbf{k}_\perp \mathbf{k}_\perp}{k_\perp^2} + \left(\frac{k_\parallel^2}{k^2} \right) \frac{(\mathbf{k} \times \hat{n})(\mathbf{k} \times \hat{n})}{k_\perp^2} \right] \cdot \tilde{\mathbf{e}}_{s'} \quad (60)$$

Here, $|\mathbf{k}| = k_n$, Ω_n represents the spherical solid angle of \mathbf{k} , and V is the volume of the cavity. A similar analysis of the magnetostatic modes gives

$$\left\langle \frac{w_{s'n}^{(\text{ms})} w_{s'n}^{(\text{ms})}}{V^{\text{ms}}} \right\rangle = \int \frac{d\Omega_k}{2\pi V} \tilde{\mathbf{e}}_s^* \cdot \left[\left(\frac{k_\perp^2}{k^2} \right) \frac{(\mathbf{k} \times \hat{n})(\mathbf{k} \times \hat{n})}{k_\perp^2} \right] \cdot \tilde{\mathbf{e}}_{s'} \quad (61)$$

The connection between the cavity case (56) and the radiation case (4) is now apparent. Specifically, we note that the factors $w_{s'n}^{(\text{em})}$ are zero mean Gaussian random variables with a correlation matrix given by (60). We can express the product $w_{s'n}^{(\text{em})} w_{s'n}^{(\text{em})}$ in terms of uncorrelated zero mean, unit width Gaussian random variables by diagonalizing the correlation matrix. We again introduce matrix notation and represent the ss' element of the product

$$\frac{w_{s'n}^{(\text{em})} w_{s'n}^{(\text{em})}}{V^{\text{em}}} = 2\sqrt{\frac{\epsilon}{\mu}} \Delta k_n \left\{ \left[\underline{G}^{\text{rad},*} \right]^{1/2} \cdot \underline{w}_n \underline{w}_n^T \cdot \left[\underline{G}^{\text{rad}} \right]^{1/2} \right\}_{ss'} \quad (62)$$

where $\underline{G}^{\text{rad}}$ is the radiation admittance matrix (7), and $\Delta k_n = \pi^2 / (k_n^2 V)$ is the mean separation between resonant wave numbers for EM modes on a cavity of volume V . By substituting (60) into (56), we have

$$Y_{ss'}^{\text{cav}} = \left\{ \sum_n \frac{2ik_0 \Delta k_n}{\pi(k_0^2 - k_n^2)} \left[\underline{G}^{\text{rad}} \right]^{1/2} \cdot \underline{w}_n \underline{w}_n^T \cdot \left[\underline{G}^{\text{rad}} \right]^{1/2} \right\}_{ss'} + B_{ss'}^{\text{ms}}(k_0) \quad (63)$$

where in the limit of a large cavity we have approximated the sum of the pairs of Gaussian random variables representing the magnetostatic contribution to the cavity admittance by their average values and using $\Delta k_n = 2\pi^2 / (Vk_n^2)$ for magnetostatic modes converted the sum to an integral

$$\begin{aligned} \sqrt{\frac{\epsilon}{\mu}} \sum_n \frac{i}{k_0} \frac{w_{s'n}^{(\text{ms})} w_{s'n}^{(\text{ms})}}{V^{\text{ms}}} &\approx \sqrt{\frac{\epsilon}{\mu}} \sum_n \frac{i}{k_0} \left\langle \frac{w_{s'n}^{(\text{ms})} w_{s'n}^{(\text{ms})}}{V^{\text{ms}}} \right\rangle \\ &= \sum_n \frac{2i}{k_0} \sqrt{\frac{\epsilon}{\mu}} \int \frac{k_n^2 \Delta k_n d\Omega_k}{(2\pi)^3} \\ &\quad \tilde{\mathbf{e}}_s^* \cdot \frac{(\mathbf{k}_{n\perp} \times \hat{n})(\mathbf{k}_{n\perp} \times \hat{n})}{k_n^2} \\ &\quad \cdot \tilde{\mathbf{e}}_{s'} \approx iB_{ss'}^{\text{ms}}(k_0). \end{aligned} \quad (64)$$

Equation (63) is the random coupling model prediction for the cavity admittance. The last steps are to replace the exact spectrum of eigenvalues, k_n^2 by a spectrum produced by RMT and to insert a loss term. We introduce a reference wave frequency and associated wave number $\omega_{\text{ref}} = k_{\text{ref}} c$, and we assume that the cavity is filled with a uniform dielectric with loss tangent $t_\delta = \epsilon_i / \epsilon_r$. Under these assumptions for frequencies close to the reference frequency, the frequency-dependent fraction

appearing in (63) can be expressed as

$$\frac{2k_0 \Delta k}{k_0^2 - k_n^2} = [\mathcal{K}_0 - \mathcal{K}_n + i\alpha]^{-1} \quad (65)$$

where

$$\mathcal{K}_0 = \frac{k_0^2 - k_{\text{ref}}^2}{2k_0 \Delta k} \approx \frac{\omega - \omega_{\text{ref}}}{\Delta\omega} \quad (66)$$

measures the deviation in frequency from the reference frequency, and $\Delta\omega = \Delta kc$ is the mean spacing in resonant frequencies. The resonant wave numbers are now represented as a set of dimensionless values

$$\mathcal{K}_n = \frac{k_n^2 - k_{\text{ref}}^2}{2k_0 \Delta k} \quad (67)$$

which by their definition have mean spacing of unity. These are then taken to be the eigenvalues of a random matrix from the GOE normalized to have mean spacing unity. Finally, the loss factor α is defined to be

$$\alpha = \frac{1}{2} t_\delta \frac{k_0}{\Delta k}. \quad (68)$$

We note that the zeros of the denominator are given by $k_0 = k_n - i\alpha$, which implies $\Im(\omega) = -\alpha \Delta\omega = -\omega_0 / (2Q)$. Thus, $\alpha = \omega_0 / (2Q \Delta\omega)$. This results in an expression analogous to those obtained in [5], [6], and [38] for the impedance matrix

$$\underline{Y}^{\text{cav}} = i \text{Im} \left\{ \underline{Y}^{\text{rad}} \right\} + \left[\underline{G}^{\text{rad}} \right]^{1/2} \cdot \underline{\xi} \cdot \left[\underline{G}^{\text{rad}} \right]^{1/2}. \quad (69)$$

Thus, we have seen that in cases of ports described by planar apertures, we can express the model cavity admittance in terms of the corresponding radiation impedance or admittance and a universal statistical matrix $\underline{\xi}$.

REFERENCES

- [1] H. A. Bethe, "Theory of diffraction by small holes," *Phys. Rev.*, vol. 66, no. 7, pp. 163–182, 1944.
- [2] R. F. Harrington and J. R. Mautz, "A generalized network formulation for aperture problems," *IEEE Trans. Antennas Propag.*, vol. AP-24, no. 6, pp. 870–873, Nov. 1976.
- [3] R. Harrington, "Resonant behavior of a small aperture backed by a conducting body," *IEEE Trans. Antennas Propag.*, vol. AP-30, no. 2, pp. 205–212, Mar. 1982.
- [4] C. Butler, Y. Rahmat-Samii, and R. Mittra, "Electromagnetic penetration through apertures in conducting surfaces," *IEEE Trans. Antennas Propag.*, vol. AP-26, no. 1, pp. 82–93, Jan. 1978.
- [5] X. Zheng, T. M. Antonsen, and E. Ott, "Statistics of impedance and scattering matrices in chaotic microwave cavities: Single channel case," *Electromagnetics*, vol. 26, p. 3, 2006.
- [6] X. Zheng, T. M. Antonsen, and E. Ott, "Statistics of impedance and scattering matrices of chaotic microwave cavities with multiple ports," *Electromagnetics*, vol. 26, p. 33, 2006.
- [7] G. Gradoni, J.-H. Yeh, B. Xiao, T. M. Antonsen, S. M. Anlage, and E. Ott, "Predicting the statistics of wave transport through chaotic cavities by the random coupling model: A review and recent progress," *Wave Motion*, vol. 51, no. 4, pp. 606–621, 2014.
- [8] V. Lomakin and E. Michielssen, "Beam transmission through periodic subwavelength hole structures," *IEEE Trans. Antennas Propag.*, vol. 55, no. 6, pp. 1564–1581, Jun. 2007.
- [9] C. Bouwkamp, "Theoretical and numerical treatment of diffraction through a circular aperture," *IEEE Trans. Antennas Propag.*, vol. AP-18, no. 2, pp. 152–176, 1970.
- [10] H. Levine and J. Schwinger, "On the theory of diffraction by an aperture in an infinite plane screen. i," *Phys. Rev.*, vol. 74, pp. 958–974, Oct. 1948.

- [11] A. Roberts, "Electromagnetic theory of diffraction by a circular aperture in a thick, perfectly conducting screen," *J. Opt. Soc. Am. A*, vol. 4, no. 10, pp. 1970–1983, Oct. 1987.
- [12] R. Kiebert and A. Ishimaru, "Aperture fields of an array of rectangular apertures," *IRE Trans. Antennas Propag.*, vol. AP-10, no. 6, pp. 663–671, Nov. 1962.
- [13] C. Cockrell, "The input admittance of the rectangular cavity-backed slot antenna," *IEEE Trans. Antennas Propag.*, vol. AP-24, no. 3, pp. 288–294, May 1976.
- [14] R. Harrington and J. Mautz, "Characteristic modes for aperture problems," *IEEE Trans. Microw. Theory Techn.*, vol. MTT-33, no. 6, pp. 500–505, Jun. 1985.
- [15] T. Wang, R. Harrington, and J. Mautz, "Electromagnetic scattering from and transmission through arbitrary apertures in conducting bodies," *IEEE Trans. Antennas Propag.*, vol. 38, no. 11, pp. 1805–1814, Nov. 1990.
- [16] Y. Rahmat-Samii and R. Mittra, "Electromagnetic coupling through small apertures in a conducting screen," *IEEE Trans. Antennas Propag.*, vol. AP-25, no. 2, pp. 180–187, Mar. 1977.
- [17] D. Hill, M. Ma, A. Ondrejka, B. Riddle, M. Crawford, and R. Johnk, "Aperture excitation of electrically large, lossy cavities," *IEEE Trans. Electromagn. Compat.*, vol. 36, no. 3, pp. 169–178, Aug. 1994.
- [18] J. Ladbury, T. Lehman, and G. Koepke, "Coupling to devices in electrically large cavities, or why classical EMC evaluation techniques are becoming obsolete," in *Proc. IEEE Int. Symp. Electromagn. Compat.*, Aug. 2002, vol. 2, pp. 648–655.
- [19] D. Fedeli, G. Gradoni, V. Primiani, and F. Moglie, "Accurate analysis of reverberation field penetration into an equipment-level enclosure," *IEEE Trans. Electromagn. Compat.*, vol. 51, no. 2, pp. 170–180, May 2009.
- [20] T. Teichmann and E. P. Wiener, "Electromagnetic field expansions in loss-free cavities excited through holes," *J. Appl. Phys.*, vol. 24, no. 3, p. 262, 1953.
- [21] H.-J. Stockmann, *Quantum Chaos*. Cambridge, U.K.: Cambridge Univ. Press, 1999.
- [22] M. L. Mehta, *Random Matrices*. New York, NY, USA: Elsevier, 2004.
- [23] S. Hemmady, X. Zheng, E. Ott, T. M. Antonsen, and S. M. Anlage, "Universal impedance fluctuations in wave chaotic systems," *Phys. Rev. Lett.*, vol. 94, p. 014102, Jan. 2005.
- [24] X. Zheng, S. Hemmady, T. M. Antonsen, S. M. Anlage, and E. Ott, "Characterization of fluctuations of impedance and scattering matrices in wave chaotic scattering," *Phys. Rev. E*, vol. 73, p. 046208, Apr. 2006.
- [25] S. Hemmady, X. Zheng, J. Hart, T. M. Antonsen, E. Ott, and S. M. Anlage, "Universal properties of two-port scattering, impedance, and admittance matrices of wave-chaotic systems," *Phys. Rev. E*, vol. 74, p. 036213, Sep. 2006.
- [26] S. Hemmady, T. Antonsen, E. Ott, and S. Anlage, "Statistical prediction and measurement of induced voltages on components within complicated enclosures: A wave-chaotic approach," *IEEE Trans. Electromagn. Compat.*, vol. 54, no. 4, pp. 758–771, Aug. 2012.
- [27] Z. Drikas, J. Gil Gil, S. Hong, T. Andreadis, J.-H. Yeh, B. Taddese, and S. Anlage, "Application of the random coupling model to electromagnetic statistics in complex enclosures," *IEEE Trans. Electromagn. Compat.*, vol. 56, no. 6, pp. 1480–1487, Dec. 2014.
- [28] C. Holloway, D. Hill, J. Ladbury, G. Koepke, and R. Garzia, "Shielding effectiveness measurements of materials using nested reverberation chambers," *IEEE Trans. Electromagn. Compat.*, vol. 45, no. 2, pp. 350–356, May 2003.
- [29] D. Hill, "Plane wave integral representation for fields in reverberation chambers," *IEEE Trans. Electromagn. Compat.*, vol. 40, no. 3, pp. 209–217, Aug. 1998.
- [30] G. Gradoni and L. Arnaut, "Higher order statistical characterization of received power fluctuations for partially coherent random fields," *IEEE Trans. Electromagn. Compat.*, vol. 51, no. 3, pp. 583–591, Aug. 2009.
- [31] M. Born and E. Wolf, *Principles of Optics: Electromagnetic Theory of Propagation, Interference and Diffraction of Light*. Cambridge, U.K.: Cambridge Univ. Press, 1999.
- [32] Z. Khan, C. Bunting, and M. D. Deshpande, "Shielding effectiveness of metallic enclosures at oblique and arbitrary polarizations," *IEEE Trans. Electromagn. Compat.*, vol. 47, no. 1, pp. 112–122, Feb. 2005.
- [33] V. Rajamani, C. Bunting, M. D. Deshpande, and Z. Khan, "Validation of modal/mom in shielding effectiveness studies of rectangular enclosures with apertures," *IEEE Trans. Electromagn. Compat.*, vol. 48, no. 2, pp. 348–353, May 2006.
- [34] G. Gradoni, T. M. Antonsen, S. Anlage, and E. Ott, "Theoretical analysis of apertures radiating inside wave chaotic cavities," in *Proc. Int. Symp. Electromagn. Compat.*, Rome, Italy, Sep. 2012, pp. 1–6.
- [35] S. Hemmady, X. Zheng, T. M. Antonsen, E. Ott, and S. M. Anlage, "Universal statistics of the scattering coefficient of chaotic microwave cavities," *Phys. Rev. E*, vol. 71, p. 056215, 2005.
- [36] L. Warne and K. Chen, "Slot apertures having depth and losses described by local transmission line theory," *IEEE Trans. Electromagn. Compat.*, vol. 32, no. 3, pp. 185–196, Aug. 1990.
- [37] J. A. Hart, T. M. Antonsen, and E. Ott, "Effect of short ray trajectories on the scattering statistics of wave chaotic systems," *Phys. Rev. E*, vol. 80, p. 041109, Oct. 2009.
- [38] T. M. Antonsen, G. Gradoni, S. Anlage, and E. Ott, "Statistical characterization of complex enclosures with distributed ports," in *Proc. IEEE Int. Symp. Electromagn. Compat.*, Long Beach, CA, USA, Aug. 2011, pp. 220–225.
- [39] J.-H. Yeh, J. A. Hart, E. Bradshaw, T. M. Antonsen, E. Ott, and S. M. Anlage, "Experimental examination of the effect of short ray trajectories in two-port wave-chaotic scattering systems," *Phys. Rev. E*, vol. 82, p. 041114, Oct. 2010.
- [40] G. Gradoni, T. M. Antonsen, and E. Ott, "Impedance and power fluctuations in linear chains of coupled wave chaotic cavities," *Phys. Rev. E*, vol. 86, p. 046204, Oct. 2012.
- [41] T. Goblick and R. Bevensee, "Variational principles and mode coupling in periodic structures," *IRE Trans. Microw. Theory Techn.*, vol. MTT-8, no. 5, pp. 500–509, Sep. 1960.



Gabriele Gradoni (M'11) was born in Ancona, Italy, in 1982. He received the M.Sc. degree in communication engineering in 2006, and the Ph.D. degree in electromagnetics and bioengineering in 2009, both from the Università Politecnica delle Marche, Ancona.

In 2008, he was a Visiting Researcher at the Time, Quantum & Electromagnetics Team of the National Physical Laboratory, Teddington, Middlesex, U.K. From 2010 to 2013, he was a Research Associate at the Institute for Research in Electronics and Applied Physics, University of Maryland, College Park, MD, USA. Since 2013, he has been a Research Fellow at the School of Mathematical Sciences, University of Nottingham, Nottingham, U.K. His research interests include semiclassical physics, random matrix theory, wave chaos, propagation through random and stratified media, as well as nanoelectronics.

Dr. Gradoni is a Member of the IEEE Electromagnetic Compatibility Society, the American Physical Society, and the Italian Electromagnetics Society. He received the URSI Commission B Young Scientist Award 2010, and the Gaetano Latmiral Prize. Since 2014, he has been the URSI Commission E Early Career Representative.



Thomas M. Antonsen (F'12) was born in Hackensack, NJ, USA, in 1950. He received the Bachelor's degree in electrical engineering in 1973, and the Master's and Ph.D. degrees in 1976 and 1977, all from Cornell University, Ithaca, NY, USA.

He was a National Research Council Postdoctoral Fellow at the Naval Research Laboratory in 1976–1977, and a Research Scientist in the Research Laboratory of Electronics at MIT from 1977 to 1980. In 1980, he moved to the University of Maryland, where he joined the Faculty of the Departments of Electrical

Engineering and Physics in 1984. He is currently a Professor of physics and the electrical and computer engineering and a Professor of electrophysics. His research interests include the theory of magnetically confined plasmas, the theory and design of high-power sources of coherent radiation, nonlinear dynamics in fluids, and the theory of the interaction of intense laser pulses and plasmas.

Dr. Antonsen has held visiting appointments at the Institute for Theoretical Physics (U.C.S.B.), the Ecole Polytechnique Federale de Lausanne, Switzerland, and the Institute de Physique Theorique, Ecole Polytechnique, Palaiseau, France. He served as the Acting Director in the Institute for Plasma Research, University of Maryland from 1998 to 2000. He was selected as a Fellow in the Division of Plasma Physics, American Physical Society in 1986. In 1999, he co-received the Robert L. Woods Award for excellence in vacuum electronics technology; and in 2003, he received the IEEE Plasma Science and Applications Award. In 2004, he was given the Outstanding Faculty Research Award of the Clark School of Engineering. In 2010, he served as the Chair in the Division of Plasma Physics, American Physical Society. He is the author and coauthor of more than 350 journal articles and a coauthor of the book *Principles of Free-electron Lasers*. He has served on the editorial board of *Physical Review Letters*, *The Physics of Fluids*, and *Comments on Plasma Physics*.



Steven M. Anlage (M'94) received the B.S. degree in physics from Rensselaer Polytechnic Institute, Troy, NY, USA, and the M.S. and Ph.D. degrees in applied physics from the California Institute of Technology, Pasadena, CA, USA. His graduate work concerned the physics and materials properties of quasicrystals. His postdoctoral work with the Beasley-Geballe-Kapitulnik Group at Stanford University (1987–1990) concentrated on high-frequency properties of high-temperature superconductors, including both basic physics and applications to tunable

microwave devices.

He is currently a Professor of Physics and a Faculty Affiliate in the Department of Electrical and Computer Engineering, University of Maryland, College Park, MD, USA. In 1990, he was appointed as an Assistant Professor of physics in the Center for Superconductivity Research, University of Maryland, then in 1997 an Associate Professor, and finally in 2002 a Full Professor of physics. He was the interim Director in the Center for Nanophysics and Advanced Materials in 2007–2009, and is a member of the Maryland NanoCenter. There his research in high-frequency superconductivity has addressed questions of the pairing state symmetry of the cuprate superconductors, the dynamics of conductivity fluctuations and vortices, and microwave applications such as superconducting negative index of refraction metamaterials. He has also developed and patented a near-field scanning microwave microscope for quantitative local measurements of electronic materials (dielectrics, semiconductors, metals, and superconductors) down to nanometer length scales.

Dr. Anlage and collaborators have developed a statistical prediction model for effects of high-power microwave signals on electronics. He is also active in the emerging field of time-reversed electromagnetics. His research is supported by the National Science Foundation, Department of Energy and DoD, and he is an active consultant to the US Government. In 2008, he was appointed as a Research Professor in the National Security Institute, Naval Postgraduate School, Monterey, CA. In 2011, he was appointed as a Research Professor at the DFG-Center for Functional Nanostructures at the Karlsruhe Institute of Technology in Germany. He has coauthored more than 150 research papers in scientific journals. He is a Member of the American Physical Society, the Optical Society of America, and the Materials Research Society.

Edward Ott (LF'11) received the B.S. degree in electrical engineering from The Cooper Union, New York, NY, USA, in 1963, and the M.S. and Ph.D. degrees in electrophysics both from Polytechnic Institute of Brooklyn, Brooklyn, NY, in 1965 and 1967, respectively.

After receiving the Ph.D. degree, he became the National Science Foundation Postdoctoral Fellow in the Department of Applied Mathematics and Theoretical Physics, Cambridge University. Following his Postdoctoral research work, he was appointed as an Assistant Professor in the Department of Electrical Engineering at Cornell University, where he eventually became a Full Professor. In 1979, he moved from Cornell University to take up his current position as a Professor of physics and electrical engineering, University of Maryland, College Park, MD, USA, where he is currently a Distinguished University Professor. His current research interest includes the area of chaos and nonlinear dynamics.